ORIGINAL PAPER

Cord blood metabolomic profiling in intrauterine growth restriction

**Donata Favretto · Erich Cosmi · Eugenio Ragazzi · Silvia Visentin · Marianna Tucci ·
Paolo Fais · Giovanni Cecchetto · Vincenzo Zanardo · Guido Viel ·
Santo Davide Ferrara**

Abstract A number of metabolic abnormalities have been observed in pregnancies complicated by intrauterine growth restriction (IUGR). Metabolic fingerprinting and clinical metabolomics have recently been proposed as tools to investigate individual phenotypes beyond genomes and proteomes and to advance hypotheses on the genesis of diseases. Non-targeted metabolomic profiling was employed to study fetal and/or placental metabolism alterations in IUGR fetuses by liquid chromatography high-resolution mass spectrometry (LC-HRMS) analysis of cord blood collected soon after birth. Samples were collected from 22 IUGR and 21 appropriate for gestational age (AGA) fetuses. Birth weight differed significantly between IUGR and AGA fetuses ($p < 0.001$). Serum samples were immediately obtained and deproteinized by mixing with methanol at room temperature and centrifugation; supernatants were lyophilized and reconstituted in water for analysis. LC-HRMS analyses were performed on an Orbitrap mass spectrometer linked to a Surveyor Plus LC. Samples were injected into a 1.0×150-mm Luna C18 column. Spectra were collected in full-scan mode at a resolution of approximately 30,000. Data were acquired over the m/z range of 50–1,000, with measurements performed in duplicate. To observe metabolic variations between the two sets of samples, LC-HRMS data were analyzed by a principal component analysis model. Many features (e.g., ionic species with specific retention times) differed between the two classes of samples: among these, the essential amino acids phenylalanine, tryptophan, and methionine were identified by comparison with available databases. Logistic regression coupled to a receiver-operating characteristic curve identified a cut-off value for phenylalanine and tryptophan, which gave excellent discrimination between IUGR and AGA fetuses. Non-targeted LC-HRMS analysis of cord blood collected at birth allowed the identification of significant differences in relative abundances of essential amino acids between IUGR and AGA fetuses, emerging as a promising tool for studying metabolic alterations.

Keywords IUGR · Metabolomics · HRMS · Essential amino acids · Tryptophan · Phenylalanine

D. Favretto (✉) · M. Tucci · P. Fais · G. Cecchetto · G. Viel ·
S. D. Ferrara
Department of Public Health and Environmental Medicine,
Forensic Toxicology and Antidoping Unit, University of Padova,
35122 Padova, Italy
e-mail: donata.favretto@unipd.it

E. Cosmi · S. Visentin
Department of Gynecological Science and Human Reproduction,
University of Padova,
35122 Padova, Italy

E. Ragazzi
Department of Pharmacology and Anesthesiology,
University of Padova,
35122 Padova, Italy

V. Zanardo
Department of Pediatrics, University of Padova,
35122 Padova, Italy

Introduction

Intrauterine growth restriction (IUGR) is defined by the American College of Obstetricians and Gynecologists [1] as an ultrasound estimated fetal weight (EFW) less than the 10th percentile for gestational age. Regulation of fetal growth is multifactorial and complex. Several factors,

including genetic (intrinsic fetal conditions) and environmental (maternal and external conditions), can lead to IUGR and to serious consequences, e.g., activation of adaptation systems leading to considerable fetal growth retardation, metabolic, neuroendocrine and cardiovascular adaptations, and early and later life consequences [2–5].

Birth weight and gestational age at birth are the most important predictors of neonatal mortality and morbidity, being responsible for 50% of preterm and 20% of term perinatal deaths [6] and determining hypoxic encephalopathy and cerebral palsy due to *intrapartum* distress and metabolic acidosis [7].

Several studies suggest that low birth weight is associated with the development of an "in utero programmed" metabolic syndrome in adult life [2, 3].

Metabolomics, and in particular "clinical metabolomics", is commonly defined as comprehensive study of all LMW metabolites (generally, <1,500 Da) expressed in tissues, organs, or organisms and aims at evaluating and/or predicting health and disease risk. The individual genome and possibly epigenetic effects influence the metabolic signatures of a candidate tissue or body fluid by environmental exposure, diet behavior, and lifestyle. An advantage of clinical metabolomics is that it adds significant new information to the individual phenotype beyond genome and proteome analysis, just by using a small amount of body fluids [8–11].

The aim of the present study was to identify fetal and/or placental metabolism abnormalities by the study of the metabolomic profile in IUGR fetuses with non-targeted metabolomic liquid chromatography high-resolution mass spectrometry (LC-HRMS) analysis of cord blood collected soon after birth, with a cohort of appropriate for gestational age (AGA) fetuses as controls.

Materials and methods

Patient selection

A longitudinal prospective study was performed from March to December 2009 in the Maternal Fetal Medicine section and Forensic Toxicology and Antidoping Unit, University of Padova. Women were enrolled in the study during third-trimester routine fetal ultrasonography performed to evaluate EFW, amniotic fluid volume, and placenta location. Intrauterine growth restriction was defined as an EFW of <10th percentile, and AGA as an EFW between the 10th and 90th percentiles, according to Italian standards for birth weight and gestational age and confirmed at birth [12]. The Ethics Committee of the University Hospital approved the study, and written informed consent was obtained from all women.

In all patients, gestational age was determined by the last menstrual period and confirmed by ultrasound in the first trimester or at 18–24 weeks of gestation. Inclusion criteria for IUGR pregnancies were: single pregnancy and neonatal weight of <10th percentile. Inclusion criteria for AGA pregnancies were: single pregnancy and birth weight between the 10th and 90th percentiles. In addition, only women undergoing cesarean section and not in labor were considered for the study, in order to exclude labor as a factor which may alter metabolomic results. Exclusion criteria for both groups were multiple pregnancies, chromosomal abnormalities or syndromes, congenital infection, preeclampsia, fetal alcohol syndrome or maternal drug ingestion, other congenital or acquired diseases leading to postnatal growth restriction (severe cardiac malformation, bronchopulmonary dysplasia, or severe malformations), and large-for-gestational-age fetuses, >90th percentile.

Clinical characteristics of study population

Maternal and neonatal characteristics are listed in Table 1. Forty-three Caucasian women met the inclusion criteria. Of these, 22 had IUGR and 21 AGA fetuses. Median maternal age at delivery was 32 years (range, 23–37) in the IUGR and 30 years (range, 24–44) in the AGA group. All women in the IUGR group were delivered by cesarean section (five for fetal distress and five for previous cesarean section) as were those in AGA group (21 for previous cesarean delivery). Median gestational age at delivery for IUGR fetuses was 38 weeks (range, 32–41.3), and median birth weight was 2,477.5 g (range, 1,395–2,378). Median gestational age in the AGA group was 38.3 weeks (range, 36.4–41.2), and median birth weight was 3,420 g (range, 2,650–4,200). There was a statistically significant difference in birth weight between the two groups ($p<0.001$). Three IUGR neonates needed NICU hospitalization for respiratory distress syndrome at delivery.

Sampling procedure

Fetal blood samples (0.5 mL) were obtained from the umbilical vein from a doubly clamped segment of the cord immediately after fetal extraction, and were collected in a Vacutainer SST II Advance (BP Diagnostic, Belliver Industrial Estate, Plymouth, UK) tube and centrifuged at $1,500 \times g$ for 10 min at 4 °C. Time from birth to sample collection did not exceed 10 min. Time was recorded with a stopwatch.

Sample preparation

Serum samples (200 μl) were immediately deproteinized by mixing with methanol (600 μl) at room temperature, vortex

Table 1 Clinical characteristics of the study population

	IUGR (n=22)	AGA (n=21)	p
Maternal age (year)	32 (23–37)	30 (24–44)	NS
Gestational age at delivery (weeks)	38 (32–41.3)	38.3 (36.4–41.2)	NS
Birthweight at delivery (g)	2,477.5 (1,395–2,378)	3,420 (2,650–4,200)	<0.001
Apgar at 5 min	9 (7–10)	9 (7–10)	NS

Data are expressed in median and range

mixed for 20 s, and incubated at −20 °C overnight. Samples were then centrifuged (13,845×g, 15 min, 4 °C). Supernatants were transferred to Eppendorf tubes and lyophilized. Samples were reconstituted in 100 μl of water prior to analysis.

Liquid chromatography coupled with high-resolution mass spectrometry analysis

LC-HRMS analysis was performed on an LTQ-orbitrap mass spectrometer (Thermo Fisher Scientific, Bremen, Germany) connected to a Surveyor Plus LC. Samples were injected into a 1.0×150-mm Luna C18 column (Phenomenex, Torrance, CA, USA). Samples were eluted at a flow rate of 0.1 mL/min, with a chromatographic gradient of two mobile phases: water, 0.1% formic acid (phase A) and methanol, 0.1% formic acid (phase B). After an isocratic step of 1 min at 90% phase A and 10% phase B, a linear gradient from 10% to 100% B was run over the next 35 min, with a mobile phase flow of 0.1 mL/min. A 10-μl sample volume was injected into the column. An electrospray source was used, working in positive ion mode. For the positive ion detection mode, the sheath gas was set at 13 (arbitrary units) and the auxiliary gas at 29 (arbitrary units), and capillary temperature was 275 °C. The spray voltage and tube lens voltage were 4,500 and 85 V, respectively. Lens parameters were optimized with a tune solution containing 14 metabolites (cystine, arginine hydrochloride, arginine, tryptophan, lysine monohydrochloride, lysine, tyrosine, serine, valine, leucine, asparagine, glutamic acid, methionine, and histidine) at a concentration of 1–3 mmol/L and infused at 5 μL/min. Gas flows were then optimized with the same compounds but with a 0.1-mL/min HPLC flow. Orbitrap calibration was performed in the positive ion mode. Spectra were collected in full-scan mode at a mass resolution of approximately 30,000 (full width at half maximum of peak, FWHM). Data were acquired over the m/z range of 50–1,000 at a speed of 0.45 s/scan (2 μscans). Measurements were performed in duplicate (two injections from the same sample), to account for any analytical variability.

All data were processed with Qualbrowser (Thermo Fisher) and its chemical formula generator was used to provide elemental compositions.

Raw data from analysis were transformed to peak tables by XCMS software (http://massspec.scripps.edu/xcms/xcms.php), including statistical tools (see below).

Statistical analysis

Data pre-processing

Raw LC/MS data were preprocessed for untargeted metabolite profiling with the open-source package XCMS [13], written in R statistical programming language, available at Metlin Metabolite Database and the Bioconductor Bioinformatics Project [14]. Peak matching and single-step retention time alignment of all samples were obtained automatically, and a matrix of aligned peaks was produced in .tsv format. Values close to zero due to baseline noise were filtered and excluded since these values can interfere with computational algorithms in further data analysis.

Peak detection was performed at a minimum peak width of 1 ppm, a noise threshold of 5, and a subtraction multiple factor of 1.5. Alignment involved a 10-ppm mass tolerance and a 0.1-min retention-time tolerance.

Any relationships between pairs of variables were tested by least squares linear regression, quantified by Pearson's correlation coefficient r, considered significant for $p<0.05$.

Univariate analysis

To identify the most significant differences between IUGR and AGA data points, univariate statistical analysis was first used. Filtering procedures, such as fold-change analysis and t tests were applied, followed by a volcano plot, with a fold-change threshold of 2 and a t test threshold of 0.1. Significantly different data at the probability level of $p<0.05$ were used for further procedures of multivariate analysis, to obtain identification of relevant biomarkers.

One-way ANOVA was used to detect differences between the two groups. Differences were judged statistically significant at $p<0.05$.

Multivariate analysis

Multivariate analysis allows the limitations of simple visual examination of spectra profiles to be overcome since it

works on the entire set of variables (i.e., the relative abundances of all ionic species detected) and often allows satisfactory exploratory analysis of the complete metabolite fingerprints of the species examined [15].

Cluster analysis In order to group spectra, cluster analysis was initially used. Various clustering algorithms, both hierarchical and non-hierarchical, running under R, were tested in a preliminary assessment of the data, such as average linkage (with centroids of measurements), complete linkage (with the farthest pair of observations from two groups), single linkage (with the nearest pair of data), Ward's method (minimizing the sum of squares of any two clusters), *k*-mean clustering, and a self-organizing map. Distance indices were determined by Euclidean distance. Hierarchical clustering was performed with the *hclust* function in R package *stat*. Results were presented as dendrograms or heat maps.

Principal Component Analysis Principal component analysis (PCA) was obtained with an R *prcomp* package, based on a single-value decomposition algorithm. The covariance matrix and standardized principal component score were selected. The first three components were considered for data

classification. Both 2D and 3D scatter plots were obtained to display the results of analysis.

Receiver-operating characteristic curve

The relationship between a true positive rate (sensitivity) and a false-positive rate (1 specificity) for various cut-off values of abundance of the examined ionic species was evaluated with the receiver-operating characteristic (ROC) curve and AUC calculation [16].

Metabolite identification

The metabolites of possible importance found by LC-HRMS spectrometry were compared with those stored in the Scripps Center for Mass Spectrometry (http://metlin.scripps.edu/), Mass Bank Database (http://www.massbank.jp/en/database.html) and Human Metabolome Database (http://www.hmdb.ca/). The identities of metabolites of particular interest were confirmed by comparison of their retention times, accurate mass spectra, and high-resolution MS/MS information to those of authentic chemical standards.
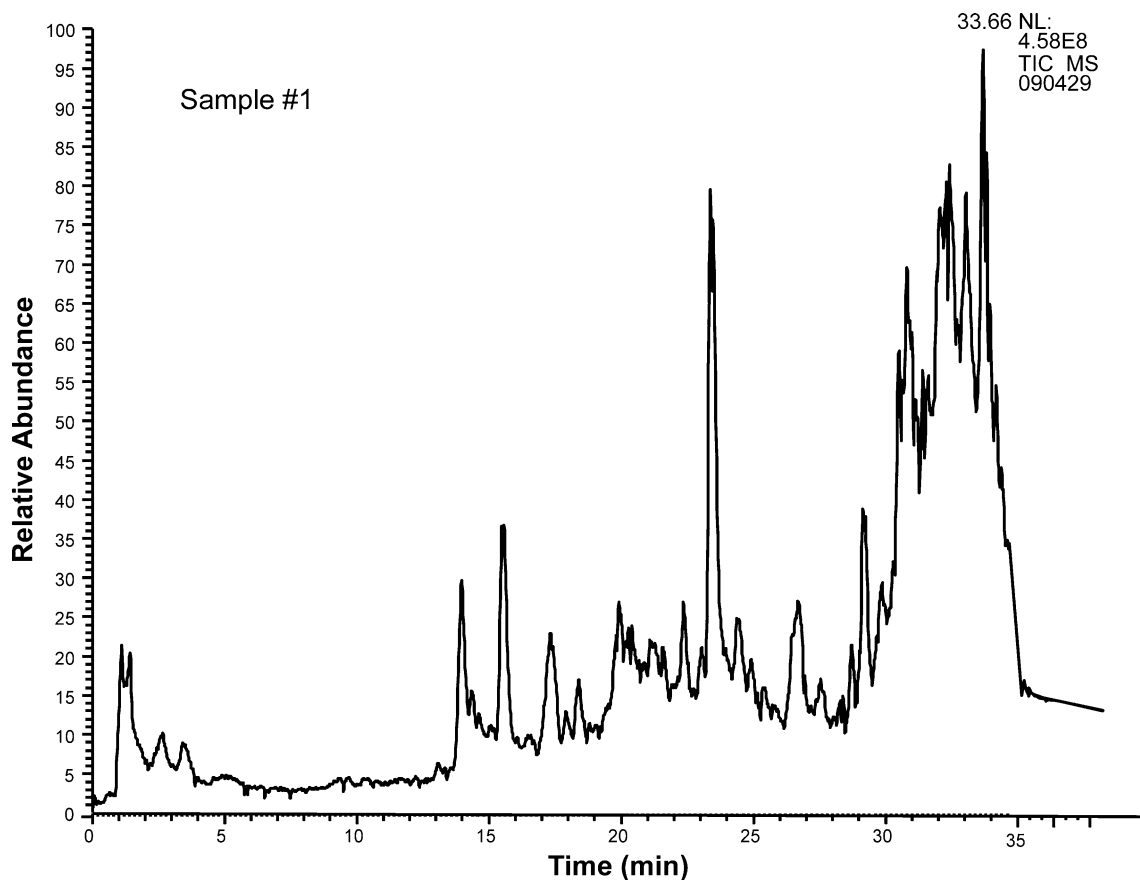

Fig. 1 Total ion chromatogram (*TIC*) obtained for IUGR sample #1

Results

LC-HRMS data

A first set of samples was analyzed in both negative and positive ion mode; the positive ion mode revealed a better sensitivity and increased the number of compounds detected. For this reason, the data from negative ion mode were not used in this study and the remaining samples were analyzed by using only positive ion detection mode. A sample of an ion chromatogram (total ion chromatogram) of one IUGR sample was reported in Fig. 1.

Ionic species profiles detected by LC-HRMS measurements revealed 864 spectral bins, which were implemented in a data matrix and statistically analyzed. Following preprocessing procedures, several species were discarded, as the algorithm used considered them within baseline noise. After filtering for this, a total of 648 ionic species remained and was subjected to multivariate analysis.

Univariate analysis

The most important features of the spectra were selected after a significant t test, fold-change analysis, and volcano plot. Most of the ionic species with their specific retention times (about 85%) were found to differ significantly between the serum samples obtained from the two classes of patients.

Multivariate analysis

Cluster analysis performed on all detected ionic species permitted to distinguish two main classes (see Fig. S1 in the Electronic supplementary material) which separated the two groups quite well. PCA analysis on the same data (Fig. 2) confirmed the trend indicated by cluster analysis: IUGR were located differently from AGA fetuses in the three-dimensional Euclidean space representing the first three principal components (explaining about 72% of total variance). Several ionic species were identified by comparison with available metabolite databases (Table 2). Focusing on these data, a simple visual inspection revealed totally different patterns of abundance in the two fetal groups (Fig. S2 in the Electronic supplementary material). The detailed distribution of the ionic species is shown in Fig. 3: all (except kynurenine and the dipeptide phenylalanyl–phenylalanine) were found to differ significantly between the two groups (ANOVA, $p < 0.0001$; for caffeine only, $p = 0.0028$). Cluster analysis of these species discriminated

Fig. 2 3D scatterplot of the first three principal components in PCA conducted on all the ionic species. The red ellipsoids are the spatial surfaces covering 50% of IUGR (blue) or AGA (red) patients, respectively. The percentage of the first three PCs responsible for the observed separation was, respectively: PC1, 54%; PC2, 10%; and PC3, 8%
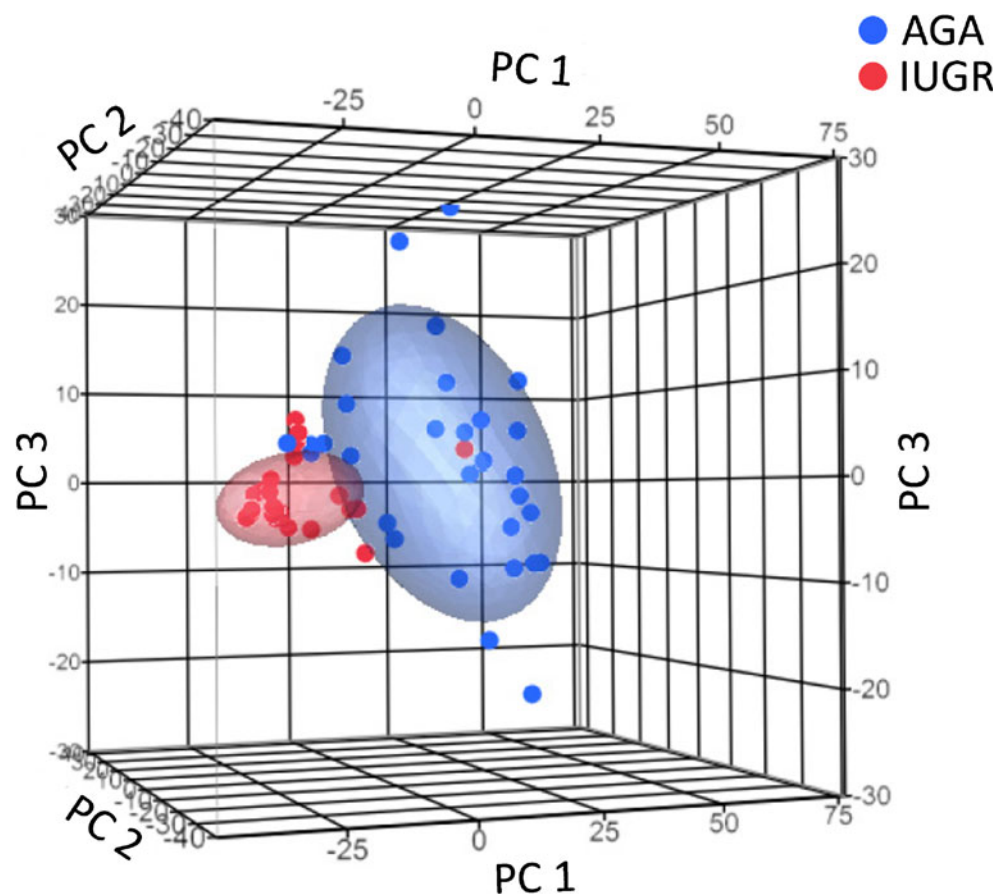
Table 2 Identified ionic species, with respective specificity and sensitivity of their diagnostic discriminant ability, obtained with ROC curve analysis

Identification type	Metabolites	Label, according to XCMS software	AUC[a]	Cut-off abundance	Specificity (%)	Sensitivity (%)
Definitive	Valine $C_5H_{11}NO_2$	M118T89	0.055556	54,334,841	96	69
Definitive	Isoleucine $C_6H_{13}NO_2$	M132T109	0.055556	183,967,098	96	69
Definitive	**Glutamate $C_5H_9NO_4$**	M148T88	0.064583	723,357	85	91
Definitive	Methionine $C_5H_{11}NO_2S$	M150T91	0.063889	747,089	96	84
Definitive	Dopamine $C_8H_{11}NO_2$	M154T113	0.065278	24,027,148	81	96
Definitive	**Hystidine $C_6H_9N_3O_2$**	M156T78	0.0625	2,616,953	71	100
Definitive	Proline $C_5H_9NO_2$	M116T89	0.054167	10,827,974	96	69
Definitive	**Phenylalanine $C_9H_{11}NO_2$**	M166T157	0.068056	118,841,665	89	100
Definitive	Uric acid $C_5H_4N_4O_3$	M169T71	0.058333	1,866,553	54	97
Definitive	Caffeine $C_8H_{10}N_4O_2$	M195T564	0.059028	4,257,749	75	81
Putative	**5-Methyl-2-undecenoic acid $C_{12}H_{22}O_2$[b]**	M199T1878	0.065278	2,474,492	96	81
Definitive	**Tryptophan $C_{11}H_{12}N_2O_2$**	M205T219	0.066667	159,059,405	86	100
Definitive	Kynurenine $C_{10}H_{12}N_2O_3$	M209T132	Nd	Nd	nd	nd
Definitive	**leu pro $C_{11}H_{20}N_2O_3$**	M229T92	0.067361	1,489,723	96	91
Definitive	L-Thyronine $C_{15}H_{15}NO_4$	M274T93	0.060417	44,019,994	96	69
Definitive	**Oleic acid $C_{18}H_{34}O_2$**	M283T1984	0.065278	1,035,372	86	94
Definitive	Hexadecanedioic acid $C_{16}H_{30}O_4$	M287T1879	0.065278	1,035,372	96	69
Putative	PHE PHE $C_{18}H_{20}N_2O_3$[b]	M313T768	Nd	Nd	nd	Nd
Putative	Arg cys asn $C_{13}H_{25}N_7O_5S$[b]	M392T1941	0.063194	1,820,121	82	97
Putative	ARG PHE ARG $C_{21}H_{35}N_9O_4$[b]	M478T2012	0.066667	5,996,730	96	84
Putative	**TRP ARG ARG $C_{23}H_{36}N_{10}O_4$[b]**	M517T1958	0.064583	14,451,441	82	100
Putative	1-Hydroxyvitamin D_3 3-D-glucopyranoside $C_{33}H_{52}O_8$[b]	M577T1978	0.061806	8,384,333	79	94

The ionic species with particular features in discriminating the two groups, suggesting relevance as markers are shown in bold

nd not determined (due to lack of fit to logistic model), *M* nominal mass, *T* retention time

[a] The area under the ROC curve (AUC) indicates the ability of the test to discriminate between subjects. An area of 1 indicates perfect accuracy with 100% sensitivity and 100% specificity; an area of 0.5 indicates casual assessment. AUC 0.90–1.00 is considered excellent, 0.80–0.90 good, 0.70–0.80 fair, 0.60–0.70 poor, and 0.50–0.60 failing. The cut-off values at various relative abundances of *m/z* were evaluated to find the best combination of sensitivity and specificity

[b] Putative metabolite did not match with the accurate mass and retention time of an authentic standard but to the accurate mass only

quite well between the two fetal groups, showing also the occurrence of a cluster among some of the ionic species (Fig. 4).

ROC curve

Logistic regression coupled with an ROC curve applied to each ionic species led to appreciable accuracy in discriminating IUGR and AGA fetuses. The area under the curve was elevated for most species, suggesting excellent accuracy in discriminating between IUGR and AGA, with high specificity and sensitivity (Table 2) at the indicated cut-offs. It should be noted that two metabolites, identified as phenylalanine and tryptophan, discriminated excellently between IUGR and AGA (specificity of 89% and 86%, respectively; sensitivity was 100% for both). As an example, logistic regression and the ROC curve for phenylalanine is shown in Fig. S3 in the Electronic supplementary material. Most of the identified metabolites were also significantly correlated, as indicated by the multiple correlations of pairwise scatter plot in Fig. S4 in the Electronic supplementary material.

Fig. 3 Box plot of the distribution of abundances of most relevant ▶ ionic species detected and identified in spectra from IUGR or AGA patients. The *ends of the box* represent the 1st and 3rd quartile, respectively. The *line across the middle of the box* indicates the median value. The *whiskers* extend from the ends of the box to the outermost data point that falls within the distances computed as (upper quartile+1.5×(interquartile range)) and (lower quartile−1.5×(interquartile range)). All data were significantly different in the two groups at *p*<0.0001 (ANOVA), except caffeine (ionic species M195T564) for which *p*=0.0028; kynurenine (M209T132) and phenylalanine–phenylalanine (M313T768) were not significantly different
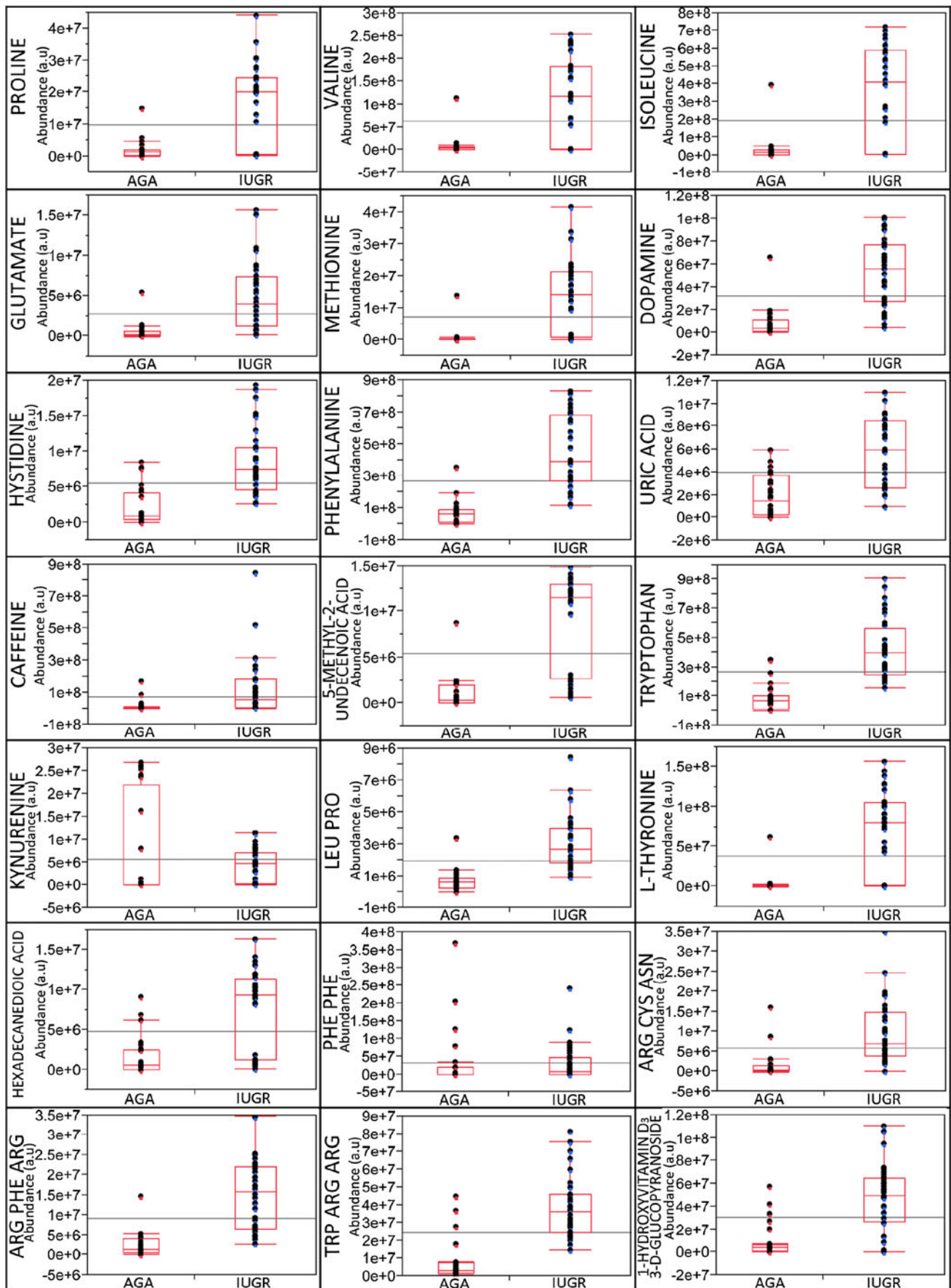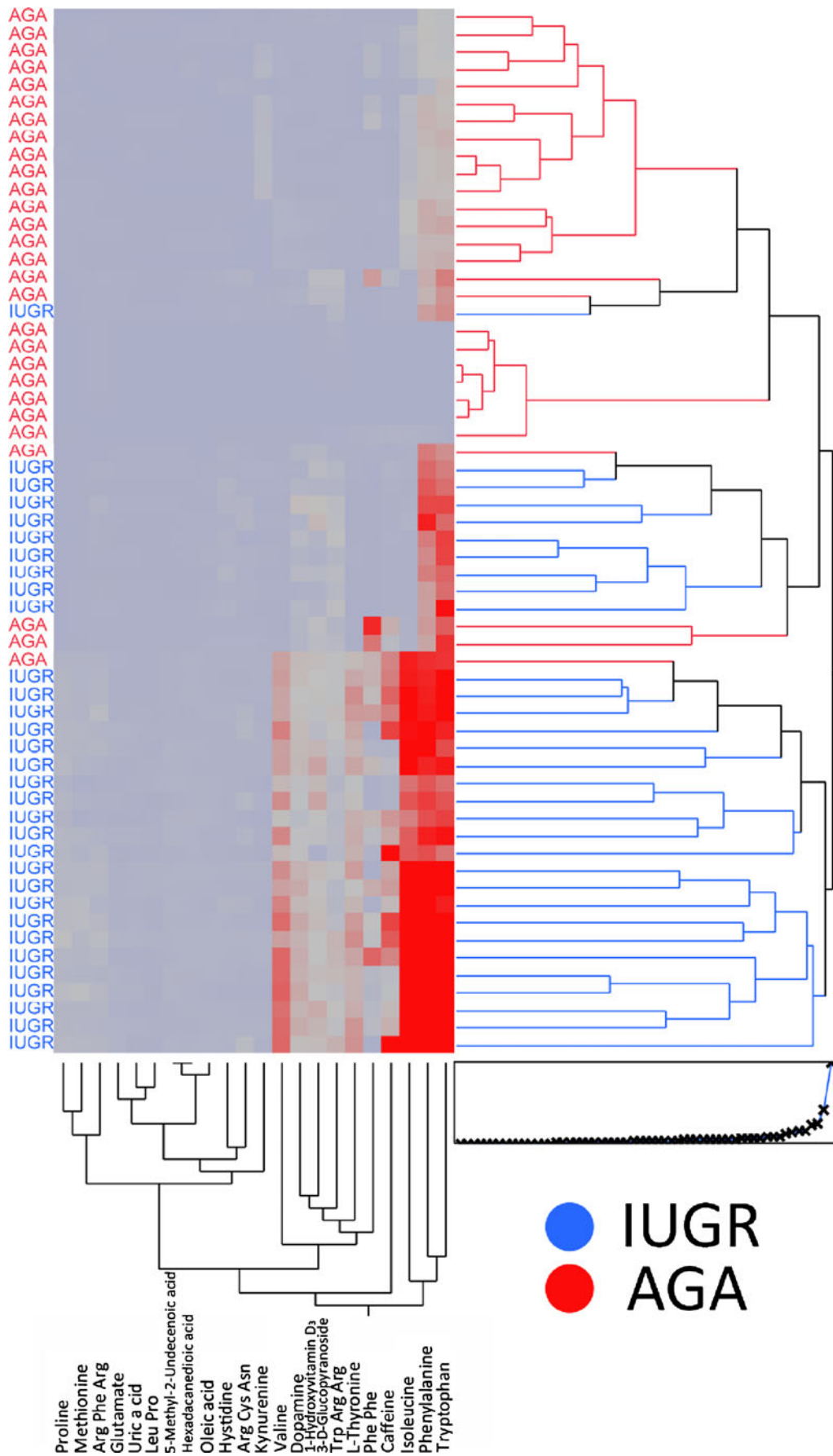
Fig. 4 Dendrogram and heatmap following cluster analysis on the 22 relevant ionic species identified in blood samples from IUGR and AGA fetuses (see Table 2). Clustering was obtained with Ward's algorithm using Euclidean distance. Abundance values for each variable are on a graduated color scale from *blue* (lower value) to *gray* to *red* (higher value). The dendrograms, provided for both patient's and metabolite's variables, show the possibility to separate quite well the two groups of patients just using the indicated metabolites. The heatmap, representing each variable's abundance with a color intensity, gives at a glance the data distribution, and makes possible to recognize that some metabolites vary more among patients, and therefore they maybe more appropriate as possible markers of disease

Discussion

It is generally accepted that IUGR is associated with a reduction in oxygen and nutrient supply across the placenta, and a number of metabolic abnormalities have been reported in pregnancies complicated by IUGR [17].

The present study highlights the fact that IUGR and AGA fetuses can be accurately discriminated according to the ionic species detected through LC-HRMS analysis in serum obtained from cord blood, which shows statistically significant differences (significant *t* test, fold-change, volcano plot and cluster analysis). In particular, 22 metabolites, identified by comparison with the available metabolomic databases (Table 2), had an excellent ability to discriminate between IUGR and AGA fetuses, measured by logistic regression analysis and an ROC curve (Fig. 3). Of these 22 metabolites, seven are alpha-amino acids. These finding were partially expected considering the recent literature evidencing the increse in essential amino acids when placental villous from small for gestational age [18] or serum from preeclampsia-diagnosed women [19] are analyzed by an analogous metabolomic strategy. However, our results are the first pertaining the cord blood metabolomic profiling, and they can help widening the knowledge of both pre-eclampsia and growth retardation phenomenon. As shown in Table 2 and Fig. 3, the best predictors (independently considered) were phenylalanine, tryptophan, and glutamate, with sensitivity ranging from 91% to 100%, and specificity between 85% and 89%. All amino acids were up-regulated in IUGR samples compared with AGA.

In humans, phenylalanine and tryptophan are both essential amino acids which must be supplied in dietary proteins. Once in the body, phenylalanine may follow any of three pathways. It may be (1) incorporated into cellular proteins, (2) converted to phenylpyruvic acid via amino acid oxidase or tyrosine amino transferase, or (3) converted to tyrosine via phenylalanine hydroxylase. Tyrosine can be converted into L-DOPA, which is further converted into dopamine, norepinephrine (noradrenaline) and epinephrine (adrenaline). Deficiencies in phenylalanine hydroxylase are responsible for the commonest form of phenylketonuria (PKU) in humans. Tryptophan functions as a biochemical precursor for serotonin, which is synthesized via tryptophan hydroxylase. Serotonin, in turn, can be converted to melatonin, via *N*-acetyltransferase and 5-hydroxyindole-*O*-methyltransferase activity. Kynurenine is the first key branch point intermediate in tryptophan's catabolic pathway, as shown in Fig. 5.

Several studies have compared the amino acid profiles of IUGR vs. AGA fetuses. Five were performed in human fetuses [20–24] and three in animals [25–27]. The most recent [18] was performed in vitro in placental tissues exposed to different O_2 tensions.

Paolini et al. [20] were the first to study amino acid placental transport in IUGR pregnancies and detected a decrease (downregulation) of phenylalanine in fetal plasma obtained after cordocentesis; they also reported lower concentrations of leucine, glycine, and proline in IUGR compared with AGA fetuses. Whereas de Boo et al. [25] reported no differences in phenylalanine and tyrosine concentrations between IUGR and AGA ewes, Morris et al. [22], in their study on free amino acid concentrations in normal and abnormal third-trimester placental villi, found increased phenylalanine in IUGR with respect to AGA humans. More recently, Horgan et al. [18] used a metabolomic approach to study the effect of changing O_2 tension on human placental metabolism in vitro, observed upregulation of amino acids (phenylalanine, tryptophan, and methionine) in small for gestational age vs. AGA conditions and suggested abnormalities in placental metabolism, amino acid transfer into fetal circulation and also feto-placental perfusion in pregnancies complicated by growth restriction. The findings of the present study, performed in vivo in fetuses from women having normal diet profiles, show that the relative concentration of phenylalanine in serum is significantly higher in IUGR than in AGA fetuses (sensitivity, 100%; specificity, 89%; Table 2) and match the results of of Horgan et al. [18]. The observed upregulation of phenylalanine may be the result of the small size of the placenta in IUGR fetuses, which in turn may lead to altered placental metabolism, with increased fetal protein catabolism and decreased amino acid transfer across the basal membrane, with a final accumulation of phenylalanine. In the study of Paolini et al. [20], in which downregulation of phenylalanine was evidenced, women were overfed with amino acid and plasma concentration ratios between the fetus and mother were recorded rather than absolute concentrations; in addition, all the IUGR fetuses had placental insufficiency and showed low pH, hypoxia, and hypercarbia during cordocentesis, which may increase the catabolic fetal status, resulting in

consumption of amino acids in different organs, particularly in the brain.

As regards tryptophan, a serotonin precursor, several reports have shown that, in rats malnourished in utero, there is an acceleration in the brain synthesis of serotonin, starting in the fetal period and coinciding with elevation of the free fraction of tryptophan in plasma and brain [28]. Increased tryptophan plasma concentrations have recently been reported also in IUGR infants [29], which suggests an increase of this serotonin precursor in the brain, with
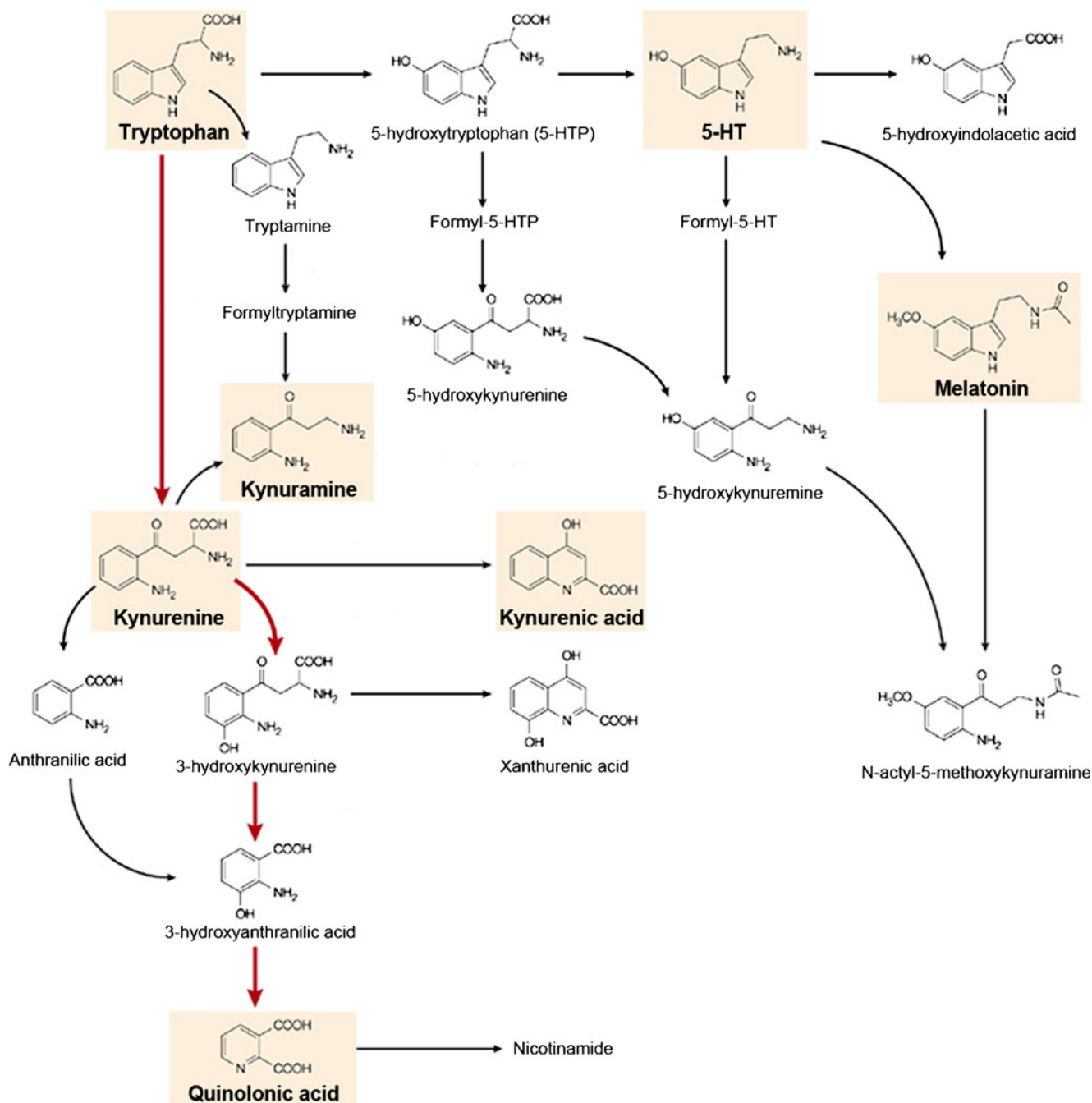

Fig. 5 Metabolism of tryptophan. Of the dietary tryptophan that is not used in protein synthesis, 99% is metabolized along the kynurenine pathway (red arrows). Alternative pathways are the conversion of tryptophan to 5-hydroxytryptamine (5-HT) and then to melatonin, or to tryptamine and then to the kynuramines (or kynurenamines). 3-HAO, 3-hydroxyanthranilic acid oxidase; IDO, indoleamine 2,3-dioxygenase; KAT, kynurenine aminotransferase; MAO, monoamine oxidase; QPRT, quinolinic-acid phosphoribosyl transferase; TDO, tryptophan 2,3-dioxygenase

enhanced serotonin synthesis and activity [30]. Huang et al. [31] located serotonin and its receptors in the placenta, implying their role in placental development. The present data unquestionably confirm that, soon after delivery, tryptophan is more concentrated in the serum of IUGR than in that of AGA fetuses.

Dunn et al. [32] and Horgan et al. [18] also noted changes in kyurenine concentrations in their studies on metabolic disturbances in placental explants in pregnancies complicated by growth restriction and/or hypoxia. We also observed lower concentrations of kynurenine in IUGR than in AGA fetuses, but this does not match the logistic model (see Fig. S3 in the Electronic supplementary material, in which only kynurenine appears to be up-regulated in AGA fetuses).

In the metabolic disruption produced in placental explants by oxygen deprivation [18], the essential amino acid methionine is up-regulated, as it was in the present in vivo study (see Table 2). Methionine has lower sensitivity (84%) but higher specificity (96%) than phenylalanine and tryptophan. Its metabolism in mammals leads to its conversion to S-adenosylmethionine (SAM) by methionine adenosyltransferase; SAM serves as a methyl donor in many methyltransferase reactions, and is converted to S-adenosylhomocysteine, in turn converted to homocysteine by adenosylhomocysteinase. Subsequently, homocysteine undergoes two fates: it can be used to regenerate methionine via methionine synthase, or to form cysteine via cystathionine-β-synthase and cystathionine-γ-lyase. Hyperhomocysteinemia has been associated with growth restriction, vasculopathies and oxidative stress [33].

Glutamate is the third amino acid with significantly different serum concentrations in IUGR and AGA fetuses, showing excellent discriminative power between the two groups of patients (sensitivity, 91%; specificity, 85%; Table 2).

The exchange of glutamate between mother and fetus is known to be important for the development of the fetus and placenta [34, 35]. The mechanisms underlying this exchange are largely unknown; however, glutamate transporters may be involved, as it is known that glutamate transporters (EAAT1, EAAT2, and EAAT3) are expressed in rat placenta [35]. It has been demonstrated by in vitro perfusion of human placenta that glutamic acid can be converted into glutamine by human placental tissue, indicating that abnormal cord concentrations of glutamate may be related to its altered placental metabolism.

In previous studies, target nutrients as well as fetal or placental metabolite concentrations have been measured by various methods at delivery in the umbilical vessels connecting the fetus to the placenta [36–41]. The proposed approach, based on untargeted metabolomic profiling, offers a more comprehensive picture of the fetal metabolome at birth, although it cannot differentiate placental metabolism from placental transport. Although presenting some limitations (e.g., small number of cases, same ethnic origin of mothers, IUGR defined here as a birth weight less than the 10th percentile), this study proposes novel and interesting insights into IUGR.

Conclusions

LC-HRMS analysis of serum obtained from cord blood collected soon after delivery revealed that the metabolic footprint in IUGR fetuses can be distinguished from that of controls and that 22 identified metabolites significantly contribute toward differentiating IUGR from AGA fetuses. To our knowledge, this is the first time that metabolomic profiling has been used to investigate IUGR in vivo. The most evident changes in the serum metabolome of IUGR fetuses were linked to amino acids; in particular, phenylalanine, tryptophan and glutamate exhibited the highest sensitivity. Our study, conducted when results from Horgan et al. [18] were not available to the scientific community, substantiate the metabolic disruption observed in vitro.

These results confirm that factors such as nutrient deficiency may play an important role in the pathophysiology of IUGR and suggest a novel point of view for investigating and perhaps understanding the pathogenesis of IUGR.

References

1. Chauhan SP, Gupta LM, Hendrix NW, Berghella V (2009) Intrauterine growth restriction: comparison of American College of Obstetricians and Gynecologists practice bulletin with other national guidelines. Am J Obstet Gynecol 200(4):e401–e406. doi:10.1016/j.ajog.2008.11.025, 409

2. Barker DJ (2006) Adult consequences of fetal growth restriction. Clin Obstet Gynecol 49(2):270–283

3. Barker DJ (2000) In utero programming of cardiovascular disease. Theriogenology 53(2):555–574

4. Baschat AA, Viscardi RM, Hussey-Gardner B, Hashmi N, Harman C (2009) Infant neurodevelopment following fetal growth restriction: relationship with antepartum surveillance parameters. Ultrasound Obstet Gynecol 33(1):44–50. doi:10.1002/uog.6286

5. Cosmi E, Visentin S, Fanelli T, Mautone AJ, Zanardo V (2009) Aortic intima media thickness in fetuses and children with intrauterine growth restriction. Obstet Gynecol 114(5):1109–1114. doi:10.1097/AOG.0b013e3181bb23d300006250-200911000-00022

6. Miller J, Turan S, Baschat AA (2008) Fetal growth restriction. Semin Perinatol 32(4):274–280. doi:10.1053/j.semperi.2008.04.010

7. Baschat AA (2010) Fetal growth restriction—from observation to intervention. J Perinat Med 38(3):239–246. doi:10.1515/JPM.2010.041

8. Lucio M, Fekete A, Weigert C, Wagele B, Zhao X, Chen J, Fritsche A, Haring HU, Schleicher ED, Xu G, Schmitt-Kopplin P, Lehmann R (2010) Insulin sensitivity is reflected by characteristic metabolic fingerprints—a Fourier transform mass spectrometric non-targeted metabolomics approach. PLoS One 5(10):e13317. doi:10.1371/journal.pone.0013317

9. Want EJ, Wilson ID, Gika H, Theodoridis G, Plumb RS, Shockcor J, Holmes E, Nicholson JK (2010) Global metabolic profiling procedures for urine using UPLC-MS. Nat Protoc 5(6):1005–1018

10. Antonucci R, Atzori L, Barberini L, Fanos V (2010) Metabolomics: the "new clinical chemistry" for personalized neonatal medicine. Minerva Pediatr 62(3 Suppl 1):145–148

11. König S (2011) Urine molecular profiling distinguishes health and disease: new ways in diagnostics? Test case UPLC-MS. Exp Rev Mol Diagn 11(4):383–391

12. Pardi G, Marconi AM, Cetin I (2002) Placental–fetal interrelationship in IUGR fetuses—a review. Placenta 23(Suppl A):S136–S141. doi:10.1053/plac.2002.0802

13. Paladini D, Rustico M, Viora E, Giani U, Bruzzese D, Campogrande M, Martinelli P (2005) Fetal size charts for the Italian population. Normative curves of head, abdomen and long bones. Prenat Diagn 25(6):456–464. doi:10.1002/pd.1158

14. Smith CA, Want EJ, O'Maille G, Abagyan R, Siuzdak G (2006) XCMS: processing mass spectrometry data for metabolite profiling using nonlinear peak alignment, matching, and identification. Anal Chem 78(3):779–787. doi:10.1021/ac051437y

15. Gentleman RC, Carey VJ, Bates DM, Bolstad B, Dettling M, Dudoit S, Ellis B, Gautier L, Ge Y, Gentry J, Hornik K, Hothorn T, Huber W, Iacus S, Irizarry R, Leisch F, Li C, Maechler M, Rossini AJ, Sawitzki G, Smith C, Smyth G, Tierney L, Yang JY, Zhang J (2004) Bioconductor: open software development for computational biology and bioinformatics. Genome Biol 5(10):R80. doi:10.1186/gb-2004-5-10-r80

16. Hanley JA, McNeil BJ (1982) The meaning and use of the area under a receiver operating characteristic (ROC) curve. Radiology 143:29–36

17. Eisen MB, Spellman PT, Brown PO, Botstein D (1998) Cluster analysis and display of genome-wide expression patterns. Proc Natl Acad Sci U S A 95(25):14863–14868

18. Horgan RP, Broadhurst DI, Dunn WB, Brown M, Heazell AE, Kell DB, Baker PN, Kenny LC (2010) Changes in the metabolic footprint of placental explant-conditioned medium cultured in different oxygen tensions from placentas of small for gestational age and normal pregnancies. Placenta 31(10):893–901. doi:10.1016/j.placenta.2010.07.002

19. Dunn WA, Broadhurst D, Brown M, Baker PN, Redman CWG, Kenny LC, Kell DB (2008) Metabolic profiling of serum using ultra performance liquid chromatography and the LTQ-Orbitrap mass spectrometry system. J Chromatogr B 871:288–298

20. Paolini CL, Marconi AM, Ronzoni S, Di Noio M, Fennessey PV, Pardi G, Battaglia FC (2001) Placental transport of leucine, phenylalanine, glycine, and proline in intrauterine growth-restricted pregnancies. J Clin Endocrinol Metab 86(11):5427–5432

21. Baioria R, Sooranna SR, Ward S, Hancock M (2002) Placenta as a link between amino acids, insulin-IGF axis, and low birth weight: evidence from twin studies. J Clin Endocrinol Metab 87(1):308–315

22. Morris NH, Burston D, Ramsay B, Sooranna SR (1995) Free amino acid concentrations in normal and abnormal third trimester placental villi. Eur J Clin Invest 25(10):796–798

23. Chien PF, Smith K, Watt PW, Scrimgeour CM, Taylor DJ, Rennie MJ (1993) Protein turnover in the human fetus studied at term using stable isotope tracer amino acids. Am J Physiol 265(1 Pt 1):E31–E35

24. Cetin I, Corbetta C, Sereni LP, Marconi AM, Bozzetti P, Pardi G, Battaglia FC (1990) Umbilical amino acid concentrations in normal and growth-retarded fetuses sampled in utero by cordocentesis. Am J Obstet Gynecol 162(1):253–261

25. De Boo HA, Van Zijl PL, Smith DE, Kulik W, Lafeber HN, Harding JE (2005) Arginine and mixed amino acids increase protein accretion in the growth-restricted and normal ovine fetus by different mechanisms. Pediatr Res 58(2):270–277. doi:10.1203/01.PDR.0000169977.48609.55

26. Bauer R, Walter B, Vorwieger G, Bergmann R, Fuchtner F, Brust P (2001) Intrauterine growth restriction induces up-regulation of cerebral aromatic amino acid decarboxylase activity in newborn piglets: [18F]fluorodopa positron emission tomographis study. Pediatr Res 49(4):474–480

27. Matsueda S, Niiyama Y (1982) The effects of excess amino acids on maintenance of pregnancy and fetal growth in rats. J Nutr Sci Vitaminol (Tokyo) 28(5):557–573

28. Hernandez RJ, Manjarrez GG, Chagoya G (1989) Newborn humans and rats malnourished in utero: free plasma L-tryptophan, neutral amino acid and brain serotonin synthesis. Brain Res 488:1–13

29. Hernandez-Rodriguez J, Meneses L, Herrera R, Manjarrez G (2009) Another abnormal trait in the serotonin metabolism path in intrauterine growth-restricted infants. Neonatology 95(2):125–131. doi:10.1159/000153096

30. Manjarrez G, Cisneros I, Herrera R, Vazquez F, Robles A, Hernandez J (2005) Prenatal impairment of brain serotonergic transmission in infants. J Pediatr 147(5):592–596. doi:10.1016/j.jpeds.2005.06.025

31. Huang WQ, Zhang CL, Di XY, Zhang RQ (1998) Studies on the localization of 5-hydroxytryptamine and its receptors in human placenta. Placenta 19(8):655–661

32. Dunn WB, Brown M, Worton SA, Crocker IP, Broadhurst D, Horgan R, Kenny LC, Baker PN, Kell DB, Heazell AE (2009) Changes in the metabolic footprint of placental explant-conditioned culture medium identifies metabolic disturbances related to hypoxia and pre-eclampsia. Placenta 30(11):974–980. doi:10.1016/j.placenta.2009.08.008

33. Aubard Y, Darodes N, Cantaloube M (2000) Hyperhomocysteinemia and pregnancy—review of our present understanding and therapeutic implications. Eur J Obstet Gynecol Reprod Biol 93(2):157–165

34. Moores RR Jr, Vaughn PR, Battaglia FC, Fennessey PV, Wilkening RB, Meschia G (1994) Glutamate metabolism in fetus and placenta of late-gestation sheep. Am J Physiol 267(1 Pt 2):R89–R96

35. Matthews JC, Beveridge MJ, Malandro MS, Rothstein JD, Campbell-Thompson M, Verlander JW, Kilberg MS, Novak DA (1998) Activity and protein localization of multiple glutamate transporters in gestation day 14 vs. day 20 rat placenta. Am J Physiol 274(3 Pt 1):C603–C614

36. Bell AW, Hay WW Jr, Ehrhardt RA (1999) Placental transport of nutrients and its implications for fetal growth. J Reprod Fertil Suppl 54:401–410

37. Grosso LM, Triche EW, Belanger K, Benowitz NL, Holford TR, Bracken MB (2006) Caffeine metabolites in umbilical cord blood, cytochrome P-450 1A2 activity, and intrauterine growth restriction. Am J Epidemiol 163(11):1035–1041. doi:10.1093/aje/kwj125

38. Jobgen WS, Ford SP, Jobgen SC, Feng CP, Hess BW, Nathanielsz PW, Li P, Wu G (2008) Baggs ewes adapt to maternal undernutrition and maintain conceptus growth by maintaining

fetal plasma concentrations of amino acids. J Anim Sci 86(4):820–826. doi:10.2527/jas.2007-0624

39. Kwon H, Ford SP, Bazer FW, Spencer TE, Nathanielsz PW, Nijland MJ, Hess BW, Wu G (2004) Maternal nutrient restriction reduces concentrations of amino acids and polyamines in ovine maternal and fetal plasma and fetal fluids. Biol Reprod 71(3):901–908. doi:10.1095/biolreprod.104.029645biolreprod.104.029645

40. Wu G, Bazer FW, Datta S, Johnson GA, Li P, Satterfield MC, Spencer TE (2008) Proline metabolism in the conceptus: implications for fetal growth and development. Amino Acids 35 (4):691–702. doi:10.1007/s00726-008-0052-7

41. Cetin I, Alvino G (2009) Intrauterine growth restriction: implications for placental metabolism and transport. A review. Placenta 30(Suppl A):S77–S82. doi:10.1016/j.placenta.2008.12.006